An Attempt to Reduce the Number of Training Samples for Convolutional Neural Networks

Yuwen Heng

Master of Science
Data Science, Technology, and Innovation
School of Informatics
University of Edinburgh
2020

Abstract

Training deep neural networks can be resources-consuming. The budget required is increasing with the growth of dataset size. During the past ten years, many achievements are dedicated to accelerating the convergence speed with heuristic or theoretical training procedures by arranging the order of training samples. However, we still need the whole dataset to train the network and paying for a large dataset may not pay back well if we can use a smaller subset to achieve an acceptable performance. In order to reduce the number of training samples needed, we first adapt three existing methods, Patterns by Ordered Projections (POP), Enhanced Global Density-based Instance Selection (EGDIS), and Curriculum Learning (CL), to reduce the size of two image datasets, CIFAR10 and CIFAR100, for the classification task. Based on the analysis, we present our main contribution: improved CL by proposing its two variations, the Weighted Curriculum Learning (WCL) and the Boundary based Weighted Curriculum Learning (BWCL). The WCL outperforms POP and EGDIS in terms of both classification accuracy and time complexity. Also, WCL and BWCL achieve comparable performance compared with CL while keeping a portion of hard examples. Besides, we design a trade-off framework for WCL to select a subset of samples according to the acceptable relative accuracy.

Acknowledgements

First and foremost, I would like to express my deepest gratitude to my supervisor, Dr Yang Cao, for offering me the opportunity to work with him on such an attracting and challenging project. His encouragement and valuable guidance helped me tackle the obstacles in my research path.

Furthermore, special thanks go to Professor Bob Fisher, Dr Pavlos Andreadis at the University of Edinburgh and Dr Jiacheng Ni at IBM for sharing me their knowledge about computer vision and deep learning. The programming skills and coursework experience that I learnt from them helped me to organise the experiments well.

Finally, I would like to send my love to my fiancee Danni Li for her accompany during the past three years. I wouldn't have the chance to study full-time without her full support.

Table of Contents

1 Introduction **1**

2 Background Research **4**

2.1 Classification and Feature Extraction with CNNs 4

2.2 Training Set Arrangement 6

2.2.1 Current Hypothesis Methods 6

2.2.2 Target Hypothesis Methods 8

2.3 Instance Selection Algorithm 9

2.3.1 Patterns by Ordered Projections 10

2.3.2 Enhanced Global Density Based Instance Selection 11

2.4 Trade-off Framework 13

3 Methods **14**

3.1 Datasets and Image Feature Extraction 15

3.2 Instance Selection Algorithms for CNNs 16

3.2.1 Weighted Curriculum Learning 16

3.2.2 Boundary Based Weighted Curriculum Learning 17

3.3 Evaluation Designs 18

4 Instance Selection Evaluation **19**

4.1 Experiment 1: Feature Extraction 19

4.2 Experiment 2: Intrinsic Behaviour 22

4.3 Experiment 3: Logistic Regression 27

4.4 Experiment 4: Instance Selection for CNN 31

4.5 Conclusion 34

5 Trade-off Framework **35**

5.1 Trade-off Framework Design 36

5.1.1 Performance Evaluation 37

6 Conclusion and Future Work **39**

Bibliography **41**

A Training History **46**

A.1 Feature Extraction for CIFAR20 and CIFAR40 46

A.2 Logistic Regression Original History 47

A.3 CNN Original History 47

Chapter 1

Introduction

With the development of Convolutional Neural Networks (CNNs), many computer vision challenges have proven to achieve high performances on image datasets. Krizhevsky et al. [25] designed an eight-layer CNN and outperformed the record in the ImageNet Large Scale Visual Recognition Competition (ILSVRC2012) by about 9.4 per cent. Three years later, the very deep CNN by He et al. [17, 18] surpassed human-level performance on the same dataset. It is possible to train CNNs with hundreds of layers due to the increment of dataset size, robust initialisation methods, development of GPU training frameworks, advanced regularisation skills, and network architectures such as highway connection [18, 19]. These achievements made deep CNNs the dominant choice for the image classification task. However, CNNs are not perfect. The training process may need to evaluate all the images for hundreds of times to achieve good accuracy in a typical workflow gradually. While deep architectures achieved high accuracies, the large-scale datasets also caused CNNs both time-consuming and eager for computing and storage resources.

In order to overcome these drawbacks, recent research developed many training data arrangement procedures to accelerate the CNN convergence speed. These approaches typically fall into one of the two categories: select mini-batch samples [1] non-uniformly [37, 27, 21, 9] or rank the order by which samples are fed into CNNs during training [5, 16]. Both methods need to evaluate sample classification scores. We have two options on when to evaluate the classification scores: at each training step or calculate once before the training process starts. We use the term **Current Hypothesis Method** and **Target Hypothesis Method** to refer to these situations [16]. However, we still need to train the whole training set or evaluate them during training.

[1] In our dissertation, we use the term samples to represent the data in datasets

There are methods designed to reduce the number of training samples which have structured features called **instance selection** algorithms [31, 3, 8, 34]. The typical approach is to select samples that can maintain the decision boundary of machine learning algorithms such as k-nearest neighbour (knn) [29]. However, to the best of our knowledge, researchers have not developed an efficient pipeline to make them work with image datasets and CNNs [39, 4, 6]. One reason is that images are not structural data. The other reason is that these selection algorithms are not designed for CNNs. Hence, we need to build a pipeline for these algorithms to be compatible with CNNs.

This project aims to establish an efficient pipeline to reduce the number of training samples needed for CNNs. We take the image classification task as an example in particular. To do so, we will adapt typical instance selection algorithms and the target hypothesis methods to reduce the size of training set for CNNs. Before CNNs became popular, researchers tend to reduce the image dimensionality by transforming the images into feature vectors then classify these features with machine learning algorithms such as SVM [33, 12]. Since these extracted features can be considered as structural features, and the pre-calculated classification scores can reflect the sample classification difficulties for CNNs, it is possible to achieve a better reduction performance, in terms of classification accuracy and algorithm operation time.

In specific, we will extract the image feature vectors as a pre-processing step. The existing instance selection algorithms are extended with the awareness of sample classification scores. Since there is no enough experience to guide us configure the algorithms for CNNs, we plan to explore the behaviours first by visualising the selected samples and train the subsets with the logistic regression method. After tuning the hyper-parameters [2] and selecting the subsets on the feature vectors, we train CNNs from scratch with corresponding images and report the relative classification accuracies [3]. We then dive into the most suitable algorithm and build the trade-off framework, which can guide researchers to balance the relative accuracy and the number of samples selected.

This dissertation is structured as follows:

Chapter 2: Background Research. We describe the necessary background to understand image classification and image feature extraction with CNNs. We briefly mention the theory for current hypothesis methods. Moreover, we describe the imple-

[2] Hyper-parameter means the parameter that we can tune by hand

[3] Relative accuracy is defined as the test set accuracy of selected subset divided by that of the whole training set.

mentations of one target hypothesis method and two instance selection methods for later evaluation. We also cover the CNN accuracy prediction method by training a regression model with existing experiment results.

Chapter 3: Methods. We introduce the datasets and feature extraction procedures used in the experiments. Based on the target hypothesis method described in Chapter 2, we propose two variations dedicated to CNNs. After that, we cover the experiments to evaluate the five instance selection algorithms by extracting image features first then run the instance selection algorithms on these feature vectors.

Chapter 4: Instance Selection Evaluation. We compare the instance selection algorithms by selecting the same number of samples and report the test set accuracy. We report our experiment results that our variations are more suitable for CNNs. The linear relationship between the selected number of samples and the relative accuracy provides a heuristic way to decide how many samples to select.

Chapter 5: Trade-off Framework. With the experiment data acquired in Chapter 4, we build a simple framework that can predict the relative accuracy of a selected subset.

Chapter 6: Conclusion and Future Work. We finish this thesis with a conclusion and a discussion about future work.

Chapter 2

Background Research

In this chapter, we begin with presenting the necessary background to understand the CNNs for image classification and feature extraction task, training data arrangement procedures, and instance selection methods, as well as other ideas required to understand our trade-off framework. We start with the typical structure of CNNs and the gradient descent training method. We then discuss the advanced training set arrangement methods that can speed up the training procedure and outline their deficiencies for our purpose. Next, we review the instance selection literature and present a CNN instance selection pipeline - use the network pre-trained on ImageNet to extract low-dimensional features and run the instance selection methods on extracted features. Furthermore, we cover the existing trade-off framework BlinkML [32] in the context of maximum-likelihood estimation machine learning algorithms and explain why it is not suitable for the deep neural network. Finally, we present TAPAS [20], which is an accuracy predictor for the deep neural networks without training and has several properties that make it useful to build our trade-off framework.

2.1 Classification and Feature Extraction with CNNs

Classification is a kind of machine learning task which learns the mapping between visual inputs and output labels from a set of well-labelled training samples. The visual data can be images, videos or even 3D models [38]. The output scores after a softmax operation can be considered as the probability for a given image belonging to each class. We use the symbol $P(c|x,\theta)$ to represent the probability that sample x belongs to true class c. The scores of true classes also reflect the difficulties for CNNs to classify the samples correctly. Higher scores indicate the samples are easier to classify

than lower score samples. CNNs are particular tools that can solve the classification task. They are a set of chained operations with trainable parameters. These parameters define the actual input-out mapping. For this reason, we use the symbol $f(x|\theta)$ to represent the output score of true class predicted by the CNNs, which takes the input x with a particular parameter set θ.

Figure 2.1 gives a basic CNN structure which is optimised to classify images as cats or dogs. It contains two convolutional (Conv) layers, one max-pooling layer and one fully connected (FC) layer. The last FC layer is a multi-class logistic regression model which maps the outputs of the max-pooling layer to the classification scores. From this perspective, we can divide the CNN structure into two parts: feature extraction part and logistic regression part. The feature extraction part performs as a black box which ideally transforms the input images to points in a lower-dimensional, linearly separable space.

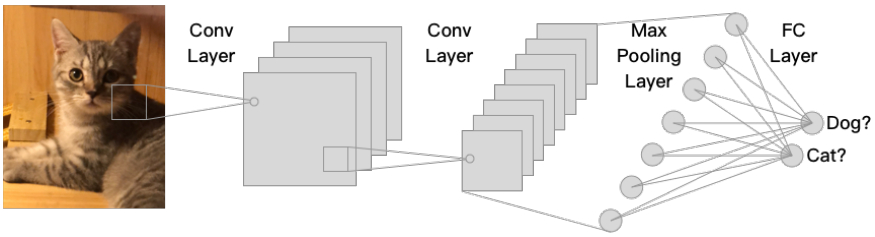

Figure 2.1: A basic CNN structure to classify images between cats and dogs. The inputs of the last FC layer are the extracted lower-dimensional features of the input images. These features should be linearly separable to achieve a high classification accuracy.

We use the symbol y to represent the ground truth of the input sample x. The equation $L(f(x|\theta),y)$ represents the loss function which measures the difference between the predicted output and the ground truth label. Then the training process is to find the parameter set θ^*, which minimise the average loss of the whole training set as follows:

$$\theta^* = \arg\min_{\theta} \frac{1}{N} \sum_{i=1}^{N} L(f(x_i|\theta), y_i) \tag{2.1}$$

where the symbol N stands for the number of samples in the training set in our dissertation. This equation turns the training process into an optimisation problem. Different from machine learning algorithms like logistic regression and SVM, the equation 2.1 is non-convex thus cannot be solved analytically [14, p. 304]. Several techniques have been developed to solve this problem with the requirement that the loss function

$L(.,.)$ is differentiable. The basic one is called stochastic gradient descent (SGD) which updates the parameters with the partial derivatives of a randomly selected sample. At each step, the new parameter is calculated with:

$$\theta_{t+1} = \theta_t - \eta \frac{\partial L(f(x|\theta), y)}{\partial \theta_t} \tag{2.2}$$

and η is the step size. A simple variant of SGD is mini-batch gradient descent which divides the training set into disjoint subsets and averages the gradients within the subset before updating the parameters:

$$\theta_{t+1} = \theta_t - \eta \frac{1}{M} \sum_{i=1}^{M} \frac{\partial L(f(x_i|\theta), y_i)}{\partial \theta_t} \tag{2.3}$$

where M is the batch size of the subset. For CNNs, batch size M is often smaller than the training set size N because it takes too much memory to fit in the whole dataset. Usually, we use the value 128 or 256 as the batch size.

The feature extraction method mentioned above is to train a network first then take the inputs of the last FC layer. In practice, this is not efficient nor effective. If we have an extensive training set, it takes us too many resources to train them well [10]. If we have a small training set, it may be hard to acquire high-quality features. An alternative method is to extract the features with a pre-trained network. Typically we use the weights trained on ImageNet [35] because this dataset is large enough and the pre-trained network can extract good enough features for other datasets [23].

2.2 Training Set Arrangement

Since the mini-batch gradient method trains the network with a subset of samples at each step, how to select the samples becomes a problem in the deep learning literature. Instead of uniform sampling, many researchers proposed to select the samples with sample weights based on different criteria. In this section, we plan to introduce the current hypothesis methods and target hypothesis methods. Current hypothesis methods measure the samples based on the parameter set θ_t at step t while target hypothesis methods are based on the final optimal parameter set θ^*.

2.2.1 Current Hypothesis Methods

Different authors have proposed a variety of current hypothesis methods. Specifically, in self-paced learning [26, 27, 30], active bias learning [9], and hard example mining

[37, 28], the batch selection process is based on the classification scores $f(x|\theta,y)$. For importance sampling methods, the process is based on the gradient norm for each sample, $|\frac{\partial L(f(x_i|\theta),y_i)}{\partial x_i}|$. We finish this section by briefly explaining the theories of these approaches [1].

2.2.1.1 Difficulty Based Methods

Self-paced learning tends to select easy samples which have a high classification score by injecting a pace function into the optimisation target function 2.1:

$$\theta^* = \arg\min_{\theta,v} \sum_{i=1}^{N} v_i L(f(x_i|\theta),y_i) + \lambda \sum_{i=1}^{N} v_i \tag{2.4}$$

where v is the sample weight calculated by the pace function. The pace function can be either a simple step function [26] or a more complicated dynamic function which changes while training [27] as long as it can assign weight 0 to samples. By minimising the target function 2.4, this method would zero out hard examples which have higher loss values, thus keeps only the easy samples. With self-paced learning, the trained network can be more robust to outliers [30].

A potential problem of self-paced learning is that it would gradually increase the loss of hard examples [26]. As a consequence, the trained network may not achieve the desired accuracy. The possible solution is to use the active bias learning method, which is designed to select the uncertain samples whose classification scores fluctuate near the decision threshold. Chang et al. proposed and evaluated many self-paced methods, and the representative one is SGD Sampled by Threshold Closeness (SGD-STC) [9]. It records the historical average classification probability $\bar{P}$ for each sample. The sample weights are calculated with an equation that is proportional to $(1-\bar{P}) \times \bar{P}$ whose maximum point is at $\bar{P} = 0.5$. However, the problem is that we need extra space and computation to maintain historical scores.

Hard example mining is yet another heuristic method aims at maximising the convergence speed by extending the self-paced learning method [37]. The algorithm proposed by [28] ranks the samples based on the latest computed classification scores in descending order. At early training stages, the algorithm chooses easy samples just like self-paced learning. After a thorough training process, the algorithm tends to select hard examples which have low classification scores. In this way, the trained classifier may be able to achieve higher accuracy than self-paced learning. The downside is that

[1] We use the term method, algorithm, approach interchangeably in this dissertation

training with hard examples can affect the decision boundary. As a consequence, the network may forget learned features previously and reduce the accuracy.

2.2.1.2 Importance Based Methods

Although experiments in the cited resources above have proved that difficulty based methods can surely speed up the training process and may achieve even higher accuracy, the lack of mathematical prove could lower the interests of researchers. On the contrary, importance based methods raise from the profound mathematical demonstration [42] and are more reliable. Despite the elaborate derivation, the most important conclusion is that the optimal weight distribution is proportional to the per-sample gradient norm.

The challenge is that computing the per sample gradient norm $|\frac{\partial L(f(x_i|\theta),y_i)}{\partial x_i}|$ is intractable. In the past few years, many researchers have adapted their approximate methods to speed up the process. The most convincing one is proposed by Katharopoulos et al. which derives an upper bound of the gradient norm [22],

$$|\frac{\partial L(f(x_i|\theta),y_i)}{\partial x_i}| \leq |h(x_i)| \tag{2.5}$$

that $h(x_i)$ is the upper bound function depends on the last layer pre-activation outputs. With this equation, we can compute the largest sample gradient after a single forward propagation.

The benefit of current hypothesis methods is that the sample weights vary with training step. Thus the chosen samples at each step can reflect the current capacity of the network. However, because evaluating the whole training set is time-consuming, we often select a subset uniformly first and then select the samples within the subset. As a result, we can only get a sub-optimal choice which is worse than the theory performance.

2.2.2 Target Hypothesis Methods

Compared with the current hypothesis methods, target hypothesis methods arrange the training set based on the possible final classification scores of the network thus the weights of the samples are pre-defined. They will not change during the training process [5]. For this reason, the target hypothesis method is more suitable to reduce the size of the datasets. To our knowledge, Curriculum Learning (CL) is the only method with these properties, as stated by Hacohen et al. in 2019 [16].

Similar to hard example mining, CL trains the network with easy samples first. Rather than switching to difficult samples, CL adds difficult samples into the training set. Eventually, the subset would contain all the training samples. The classification scores are measured with a pre-trained network or with a linear classifier such as SVM [16]. The major concern is that CL weights may not reflect the sample classification difficulties of the chosen CNN. Considering the reality that all methods described above are sub-optimal in practice, we choose to accept the drawbacks in this project.

The Python style [2] pseudo-code of CL is shown in Algorithm 1. In this dissertation, we assume the type of input feature vector is NumPy array. We make CL to select a given number of samples only once in line 5.

Algorithm 1: CL

Data: image feature vectors *M*

Input: number of samples to select *m*, classification score for each sample *scores*, number of classes *n*

Output: selected sample index by CL

```
1 selected_idx_list = [] ;
2 foreach class label L do
3 |   scores = all sample scores with label L ;
4 |   idx_list = sort_by_value(scores) ;
5 |   selected_idx_list.append(idx_list[: floor(m/n)]) ;
6 end
7 return selected_idx_list ;
```

2.3 Instance Selection Algorithm

Most instance selection methods are designed to reduce the size of the structured dataset for machine learning algorithms such as SVM and logistic regression. The assumption is that we can recover the decision boundary [3] with fewer samples. According to the thorough review [31], the instance selection methods can be divided into two categories: wrapper and filter. Wrapper methods select the subset samples based on the classification accuracy. The model knn [3] is a common choice to evaluate the classification quality. Misclassified samples will be selected because they can contribute to the knn accuracy. On the other hand, filter methods select samples without

[2] We use Python objects and their functions such as .append(). All variables ended with the postfix *_list* are Python list objects.

[3] Decision boundary is the line separates samples from different classes

repetitive evaluation. They tend to select samples near the boundary between different classes with the assumption that these samples can guide the classifiers to recover the position of the original decision boundary [34, 29]. Although the wrapper methods could achieve higher accuracy because they are classifier dependent, they tend to cost too much time because they need to evaluate the accuracy multiple times. From this perspective, filter methods are more suitable for our experiments. In this section, we take two typical filter algorithms, POP and EGDIS, to introduce their mechanisms.

2.3.1 Patterns by Ordered Projections

The POP algorithm [34] is designed to select boundary samples by removing inner samples which are far from the class contours. Rather than calculating the sample positions in the high dimensional feature space, Riquelme et al. simplified this process by projecting the samples onto each feature dimension. To be precise, we decide if a sample is inner or not in each feature space. We use the term **pure inner samples** to refer to samples which are inner in all feature dimensions.

Algorithm 2 describes the POP pseudo-code. we use the variable *weakness* to count the number of times that a sample is inner. In each feature dimension, the function *sort_by_value* first sorts the samples in descending order. Since our extracted features are continuous values, we need an extra hyper-parameter *equal* $tolerance(et)$ to decide when two feature values are equal. Then the function *resort_by_label* scans the samples and record the start label of consecutive samples with the same value and detects the label of the first sample with a different value. Then the function sorts the scanned samples by moving samples with the same labels as the two recorded to the start of the list and the end of the list. After that, we scan all samples one more time to detect label changes and mark all samples as inner except the two at the beginning and the end of the scanned list. Figure 2.2 depicts a typical work flow of POP.

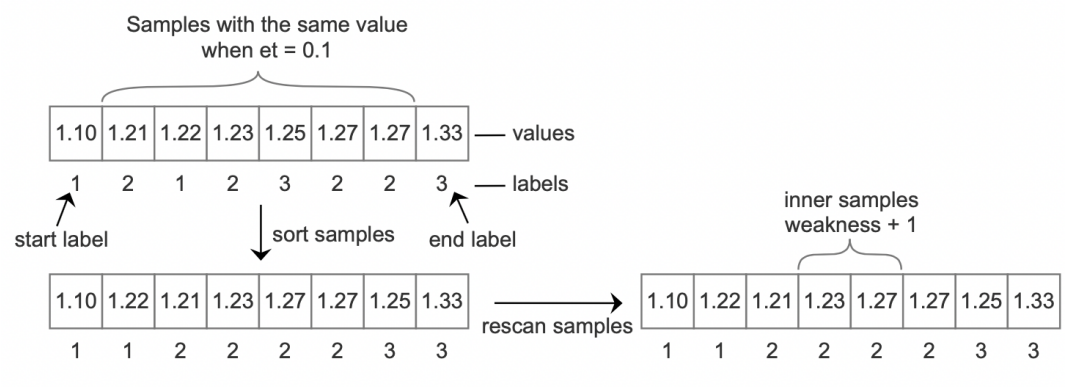

Figure 2.2: The typical workflow of POP after sorting the samples in descending order. Samples with labels 1 and 3 are not inner samples because there are only two of them.

Algorithm 2: POP for continuous features

Data: feature vectors M

Input: weakness threshold wt [a], equal tolerance et

Output: selected sample index by POP

```
weakness = np.zeros(len(M)) ;
foreach feature dimension F_j = M[:, j] do
    idx_list = sort_by_value(F_j) ;
    idx_list = resort_by_label(F_j, et, idx_list) ;
    foreach idx in idx_list do
        if M[idx, j] is inner then
            weakness[idx] += 1;
        end
    end
end
return np.argwhere(weakness < wt) ;
```

[a] Weakness threshold is equal to or smaller than the number of dimensions.

2.3.2 Enhanced Global Density Based Instance Selection

Similar to POP, EGDIS [29] aims at selecting boundary samples as well. Instead of removing inner samples, EGDIS selects the boundary samples which are close to other classes. It also selects samples at the densest area to capture some inner samples. The pseudo-code is shown in Algorithm 3. In order to find these samples, the function *kneighbours* returns the distances and labels of the k nearest neighbours. Then for each

sample, we check how many neighbours are from other classes and save the value to variable *irrelevance score*. If the score is greater than or equal to the integer part of $k/2$, we record this sample to the *boundary_idx* list. If not, function *density* calculates the global density values:

$$density(x_i) = -\frac{1}{N}\sum_{j \neq i} distance(x_i, x_j) \tag{2.6}$$

for the sample and its k neighbours. We add the sample to the *densest_idx* list if its density value is the highest compared with its k neighbours. According to the original paper, EGDIS performs better with global density function in terms of reduction rate [4]. However, the computation time increases with the number of samples in the dataset. We will explore possible solutions in Chapter 3.

Algorithm 3: EGDIS

Data: feature vectors M

Input: number of neighbourhoods k

Output: selected sample index by EGDIS

```
boundary_idx = [] ;
densest_idx = [] ;
neighbour_distance_list, neighbour_index_list = kneighbours(M, k) ;
for i in range(len(neighbour_index_list)) do
    neighbour_index = neighbour_index_list[i, :] ;
    irrelevance_score = irrelevance(neighbour_index) ;
    if irrelevance_score is greater or equal to floor(k/2) then
        boundary_idx.append(k) ;
    else
        if density(M[i]) is larger than density(M[neighbour_index]) then
            densest_idx.append(i)
        end
    end
end
return np.union1d(boundary_idx, densest_idx) ;
```

[4] Reduction rate is the percentage of samples deleted

2.4 Trade-off Framework

The main drawback of the instance selection algorithms is that we cannot control how much data to select nor the minimum accuracy [5] that we can accept. Although there is one trade-off framework published by Park et al. [32] called BlinkML, it can only work with for machine learning algorithms which can be optimised by the maximum likelihood method. Therefore, to work with CNNs, we need to build a new trade-off framework. We measure how the test set accuracy is affected by defining the relative accuracy as below:

$$Relative\ accuracy = \frac{Test\ set\ accuracy\ by\ training\ the\ selected\ subset}{Test\ set\ accuracy\ by\ training\ the\ whole\ training\ set} \tag{2.7}$$

In order to build the framework, the primary challenge is to find the relationship between required relative accuracy and the number of training samples needed. However, this is not straightforward because the optimisation of CNNs for classification tasks can be considered as a non-convex problem in most cases [15, p. 114]. It is hard to get the final accuracy without a long time training. Some second-order method could find the zero gradient point, such as Newton's method [41]. However, they are still prone to local minimum points and do not scale well to large CNNs [15, p. 310]. For the reasons mentioned above, we tend to investigate experimental methods rather than analytical methods.

In 2019, Istrate et al. published a paper aiming at predicting the accuracy without training the networks [20]. They built a Lifelong Database of Experiments (LDE) which stores a massive amount of training experiments on many CNN structures and datasets. When a new dataset is given, the framework TAPAS first train the data with a small probe CNN [36] for five epochs. The accuracy is recorded as the Dataset Characterisation Number (DCN). TAPAS then fetches experiments with similar DCN from the LDE. With these history data, a regression model is trained, which takes the network structure and DCN as inputs to predict the classification accuracies. Although it is not realistic for us to collect enough data for such a framework, TAPAS provides a working example that it is possible to build the trade-off framework based on experiment histories.

[5] Here we assume that reduce the number of samples would affect the classification accuracy, which is true from our CNN experiments.

Chapter 3

Methods

This chapter aims at describing the experiment detail to evaluate instance selection algorithms. We begin by presenting the experimental datasets, CIFAR10 and CIFAR100 [24], along with the image feature extraction process. Next, we adapt the two instance selection algorithms, POP [34] and EGDIS [29], overviewed in Chapter 2.3, together with CL [16] described in Chapter 2.2.2, to propose two instance selection methods for CNNs. We name the two methods Weighted Curriculum Learning (WCL), based on CL scores and Boundary Based Weighted Curriculum Learning (BWCL), based on the EGDIS selected boundary instances. After that, our work is focused on the comprehensive evaluation of these methods. In order to understand the behaviour of these algorithms, we first visualise the instance selection geometry patterns with CIFAR10. Then we describe the model fitting procedure for the logistic regression algorithm to choose the hyper-parameters. Finally, we extend the selection pipeline to deep learning method with the particular network, DenseNet121 [19]. Figure 3.1 gives the pipeline overview of this project. The trade-off framework is described in Chapter 5 because it is built on the evaluation results.

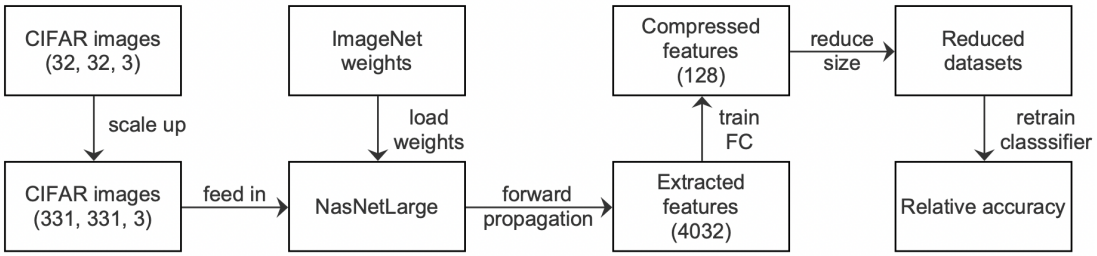

Figure 3.1: Overview of the data reduction pipeline.

3.1 Datasets and Image Feature Extraction

We choose to use CIFAR10 and CIFAR100 [24] as our experimental datasets which contain 6,000 and 600 tiny images per class respectively. Their image size is 32×32. An advantage of CIFAR is that they are plentiful in the number of images and tiny in the size of images. With CIFAR datasets, we could train the network faster, thus explore the reduction rate for a broader scale within the limited period. Another benefit is that CIFAR datasets can reflect the performance of instance selection algorithms for both simple dataset and hard dataset in term of classification accuracy. According to Kornblith et al. [23], the test set results indicate that CIFAR10 is very easy to classify and CIFAR100 is as difficult as other high-resolution datasets such as the Describable Textures Dataset (DTD) [11], Food-101 [7]. These features could gain us thorough and representative evaluation results with limited compute resources.

We performed the feature extraction task after scaling up the image size to 331 and transformed the images into range 0 to 1 by dividing 255. The goal was to provide structural features for the instance selection algorithms. We did this job with the pre-trained NasNetLarge [43] because Kornblith et al. [23] have evaluated the extracted features, and the quality is good enough. Their experiments show that the classification scores with simple logistic regression are very close to the state-of-art classification scores with CNNs. In order to simplify the implementation, we chose to use the Keras implemented NasNetLarge network downloaded from TensorFlow Hub, which is designed to get feature vectors from images [2]. However, the original shape of the feature vector is 4032, and it would take a longer time to run the instance selection algorithms. To speed up the selection process, we trained another network with two FC layers. The depth of the first FC layer is 128, and we took the outputs as compressed feature vectors. After training these two layers, the test set accuracies are reported as the baseline performance for logistic regression experiments. Figure 3.2 shows the network structure described above. We also trained a batch normalisation layer after the 128-D FC layer to limit the feature ranges. This process ensured that dimensions with a wider range would not dominate the Euclidean distance between two vectors. The KNN based algorithm, EGDIS, could work better by weighting the feature dimensions equally.

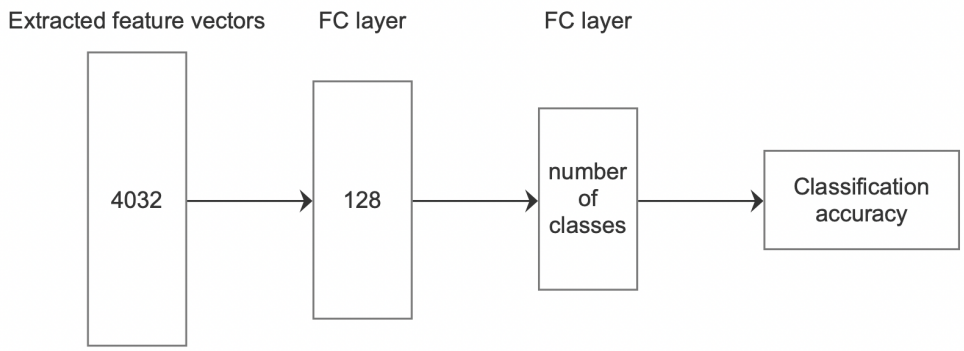

Figure 3.2: Network structure to compress the extracted feature vectors from 4032-D to 128-D. The compressed features are taken from the outputs of the first FC layer.

3.2 Instance Selection Algorithms for CNNs

Before presenting the evaluation plans, it should be noted that the algorithms described in Chapter 2 are not perfect. First of all, POP and EGDIS are not deep learning dedicated algorithms so the CNNs may not work well with selected samples. Also, although CL is a target hypothesis algorithm, only keeping easy samples may limit the highest performance that the network could achieve. Therefore, our first contribution is to enhance CL with the ability to contain a proportion of relatively difficult samples. We followed the requirement in [16] to select balanced class subsets and proposed two variations:

1. Weighted Curriculum Learning, which selects samples with the probabilities proportional to classification scores.

2. Boundary Based Weighted Curriculum Learning, which selects a proportion of the EGDIS boundary samples first then fill in the subset with WCL selected samples.

3.2.1 Weighted Curriculum Learning

In order to make CL select hard examples as well, we normalised the classification scores as the survival probabilities. By dividing the sample score to the sum of all scores, the sum of all normalised scores will be one so that we can treat them as a probability. In this way, the samples with higher classification scores would have a higher chance to be selected. Because we only selected the subset once, we should be

able to achieve higher accuracy if the network is powerful enough to learn from these hard examples. The advantage is that WCL is a self-adaptive algorithm, which can adjust the selection pattern based on how hard a dataset is. For easier datasets, WCL would select more simple samples, and for harder datasets, WCL tends to mine more hard samples. However, if the network is not capable of handling these hard examples, then the test accuracy may decay. Algorithm 4 describes the working flow in pseudo-code. The only difference compared with Algorithm 1 is the weighted selection process in line 4 and 5.

Algorithm 4: WCL

Data: feature vectors M

Input: number of samples to select m, classification score list for each sample $scores$, number of classes n

Output: selected sample index by WCL

```
1 selected_idx_list = [] ;
2 foreach class label L do
3 |   scores = all sample scores with label L ;
4 |   scores = scores / np.sum(scores) ;
5 |   idx_list = choose floor(m/n) samples based on scores ;
6 |   selected_idx_list.append(idx_list)) ;
7 end
8 return selected_idx_list ;
```

3.2.2 Boundary Based Weighted Curriculum Learning

While the score distribution of WCL selected samples can reflect the difficulty of a dataset, it cannot guarantee to select enough hard examples for the network to recognise the image patterns. Also, we planed to explore how the hard samples may affect CNN performance. Therefore, we proposed the Boundary Based Weighted Curriculum Learning to tune the number of difficult samples in the selected subset. The BWCL pseudo-code is shown in Algorithm 5. We use the parameter p to control how much EGDIS boundary samples to keep for each class. After selecting the required amount of boundary samples randomly, BWCL calls WCL to choose the rest samples from non-EGDIS boundary sample list.

Algorithm 5: BWCL

Data: feature vectors M

Input: number of samples to select m, classification score for each sample *scores*, number of classes n, EGDIS boundary sample index list $egdis\_boundary\_index$, percent of boundary to select p

Output: selected sample index by BWCL

```
selected_idx_list = [] ;
foreach class label L do
    scores = all non-EGDIS boundary sample scores with label L ;
    egdis_boundary_index_L = all EGDIS boundary sample index with label L ;
    egdis_idx = choose floor(m/n × p) samples from egdis_boundary_index_L ;
    selected_idx_list.append(egdis_idx)) ;
    scores = scores / np.sum(scores) ;
    idx_list = choose floor(m/n× (1-p)) samples with WCL from variable scores ;
    selected_idx_list.append(idx_list)) ;
end
return selected_idx_list ;
```

3.3 Evaluation Designs

We designed the following experiments to evaluate the performance of the chosen three instance selection algorithms as well as the two proposed algorithms:

1. We extracted the feature vectors for CIFAR10 and CIFAR100. We visualised the extracted features with t-SNE [40].

2. We took CIFAR10 as an example to explore the intrinsic behaviours and extraction time.

3. We reported the test set accuracy by training the selected subsets with a logistic regression model.

4. We transferred the experience gained form logistic regression experiment to evaluate the algorithm performance with the particular network, DenseNet121.

Chapter 4

Instance Selection Evaluation

We tested five algorithms to reduce the number of training samples for CNNs in this Chapter. To help the readers get the main results, we summarised our results before diving into the experiment details. First, all five algorithms are efficient for logistic regression classifier. POP is the most suitable one because it is fast and can achieve higher relative accuracy than the other four algorithms. For CNNs, we should choose CL or WCL for the reason that they do not need extra calculation and can achieve higher relative accuracy than BWCL.

4.1 Experiment 1: Feature Extraction

The python version CIFAR10 and CIFAR100 datasets are downloaded from the official website with pre-defined training and test sets [24]. In order to prevent overfitting, the training set was randomly split into training and validation sets with the ratio 8:2. We got 40,000 training samples, 10,000 validation samples and 10,000 test samples for both datasets. To speed up the experiments, we started by extracting the image feature vectors with a single forward propagation before training the FC layers.

All trainable parameters of the two FC layers were initialised by the Xavier uniform method [13]. After each epoch, we reported the validation accuracy and kept a record of the model parameters, which achieved the best validation accuracy so far. We scheduled two training stages to approach the optimal classification accuracy. First, we performed 500 training epochs with step size 0.01 then decreased it to 0.001 for another 500 epochs. After each training stage, the recorded parameters were loaded. The final held-out test set accuracy for CIFAR10 is 0.9258 and for CIFAR100 is 0.7444. Finally, we compressed the extracted 4032-D feature vectors with the 128-D FC layer.

We further took a closer look at the compressed features by projecting them down to two-dimensional vectors with t-SNE [40] which maintained the relative distance between samples. The plots are shown in Figure 4.1. Different colours represent different classes of samples. First of all, the network transformed the images into blobs. Ideally, vectors from the same class should be closer to each other. This situation is true especially for CIFAR10. Also, the quality of these compact blobs reflects the classification accuracy. Strays far from the right cluster would be misclassified by the logistic regression model, thus lower the classification accuracy.

Furthermore, the boundaries between different classes are not always clear. Some blobs are close to each other thus the classification accuracy is sensitive to slight variations of the boundary. This effect is more obvious if there are more samples for each class. The close distance between blobs partly explains the rapid vibration of the CIFAR10 validation accuracy curve shown in Figure 4.2(a). We can widen the distance between adjacent blobs by fine-tuning the pre-trained feature extraction network and achieve a higher classification score [23]. However, since we want to minimise the pre-processing time required, we omitted this step and stayed with the sub-optimal compressed features.

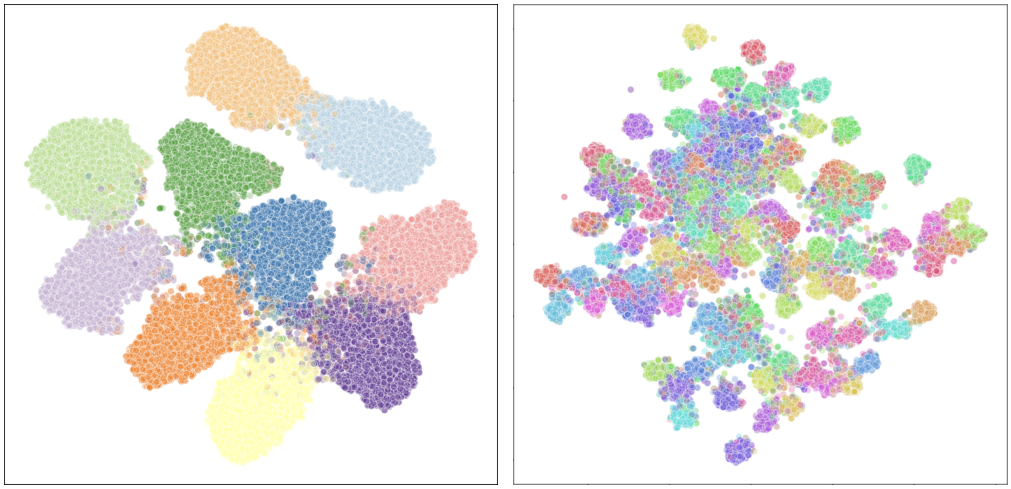

(a) CIFAR10 (b) CIFAR100

Figure 4.1: Visualisation of extracted features with the t-SNE algorithm.We can see that CIFAR10 plot is more discriminative.

In addition, we compared the training process of the two datasets in Figure 4.2. Across the two training stages, CIFAR10 converges faster than CIFAR100, but it starts to overfit earlier. The green line indicates that we could reduce the number of epochs

in the first training stage by half and leave the mining job at the second stage.

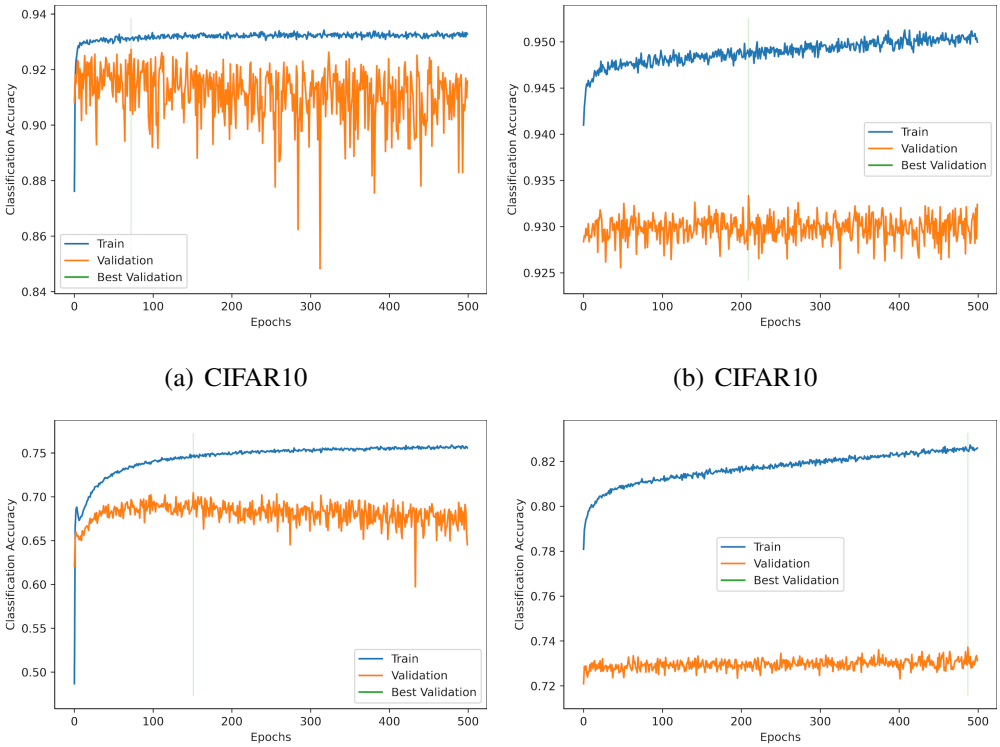

(a) CIFAR10 (b) CIFAR10

(c) CIFAR100 (d) CIFAR100

Figure 4.2: The training history of CIFAR10 and CIFAR100. The left column is the first 500 epochs and the right column is the second 500 columns. The green line represents the best validation epoch.

Finally, we also visualised the classification score distributions in Figure 4.3. As observed from the quality of blobs plotted in Figure 4.1, CIFAR10 samples tend to achieve higher classification scores around 0.9, while CIFAR100 samples are spread across the range below 0.9. A conclusion is that samples from CIFAR100 are harder to classify correctly. For this reason, we may need more samples for CIFAR100 to achieve a similar relative accuracy compared with CIFAR10. The distributions also suggest that instance selection algorithms may be less efficient for datasets with more classes and lower classification accuracies. We will discuss the algorithm performance further in Section 4.3 and 4.4.

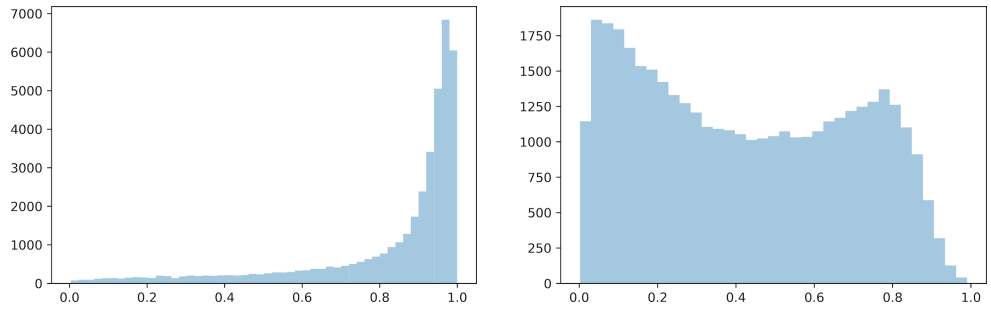

(a) CIFAR10 (b) CIFAR100

Figure 4.3: Classification score distributions. The X axis is the sample score and the Y axis is the count of samples.

4.2 Experiment 2: Intrinsic Behaviour

Obtaining the discriminative t-SNE plots, we assumed the FC layers to have learnt high quality compressed features. In this experiment, we tried to get an understanding of the intrinsic behaviours of these data reduction algorithms by visualising the selected CIFAR10 samples with red points. We managed to explain the behaviours with the answers to two questions:

1. What are the geometrical distributions of the selected samples?

2. What are the classification score distributions of the selected samples?

For each algorithm, the selection behaviours were further explored by tuning the hyper-parameters. We chose to use CIFAR10 for the reason that the quality of t-SNE projected blobs is more discriminative than CIFAR100 so that we can understand the behaviours easily.

First of all, we presented the POP selected samples by adjusting the equal tolerance of the *resort_by_label* function described in Algorithm 2. For each tolerance choice, we removed only pure inner samples whose weakness values are 128. Figure 4.4 depicts that with proper threshold setting such as $et = 1$, we can select most samples along the blob contours as desired. Also, from Figure 4.4(a) and 4.4(b), we observed a trend to select samples closer to the boundary between two adjacent blobs rather than cover the whole contours. This behaviour can guide linear classifiers to build proper decision boundaries. Another advantage of POP is fast computation speed. It took us 33.27 seconds on average to get the result. However, POP was designed to process integer features in the original paper. It is not easy to choose the suitable tolerance

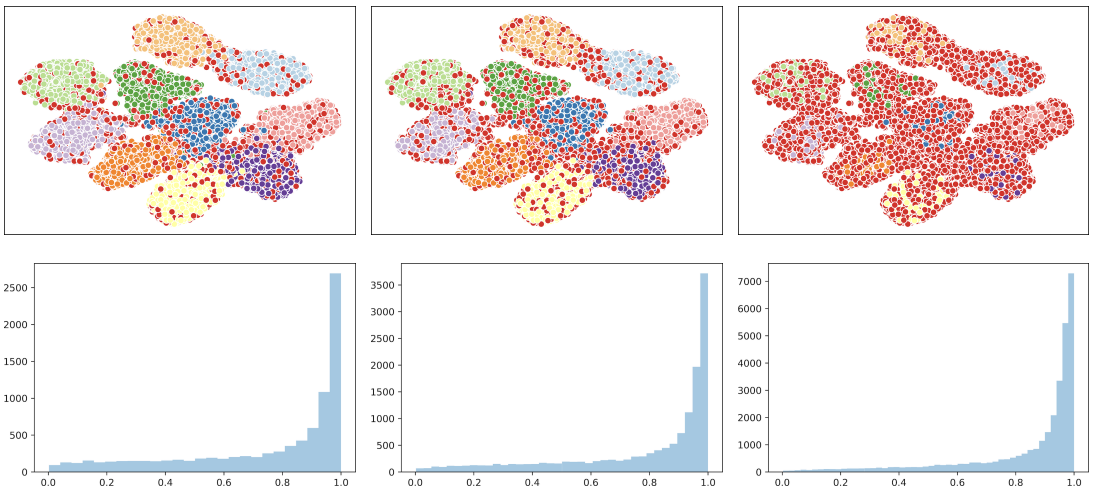

(a) et=1, 8701 samples, 33.3s (b) et=0.5, 14111 samples, 29.7s (c) et=0.1, 31966 samples, 36.8s

Figure 4.4: POP selected samples by tuning the equal tolerance. The second row is the corresponding score distributions which are similar to the dataset score distributions in Figure 4.3.

value and keep just enough samples. Our experiments indicated that the number of samples far from the boundary decreases much faster than expected by increasing the tolerance value. One possible reason is that we normalised the compressed features, and the value range is too compact. As a consequence, POP is hard to use for image datasets.

The second algorithm we explored is EGDIS by tuning the hyper-parameter k of the knn classifier. Figure 4.5 presents how the selection pattern varies with k values 3, 5, and 7. Our first discovery is that EGDIS tends to select all misclassified samples together with samples surrounding them. Compared with Figure 4.1, only a few samples still exist in different colours. Also, by increasing the value of k, fewer inner samples and boundary are selected. To explain these results, we need to know how EGDIS works with hyper-parameter k. In short, higher k values require boundary samples to have more neighbours from different classes. Based on this mechanism, we can infer that most misplaced samples are alone and surrounded by correctly classified samples. For these isolated misclassified samples, they would be considered as boundary samples and have enough number of neighbours to be selected. For samples near the boundary, fewer samples will be qualified, and only those closely contacted with other blobs would be selected. For dense samples near isolated misplaced points, some of them may be categorised as boundary samples and would not be selected anymore with an increase of k.

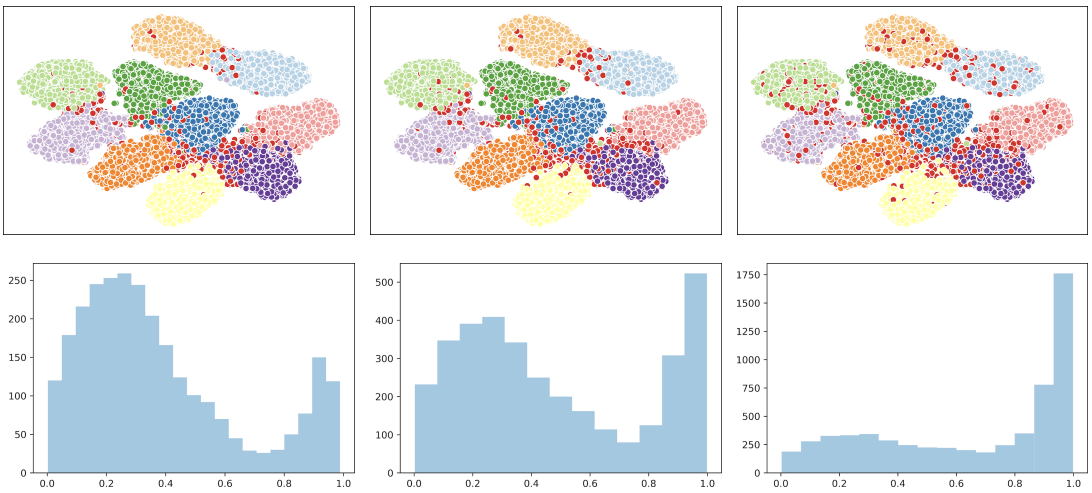

(a) k=7, 2799 samples, 14min 27s (b) k=5, 3483 samples, 15min 7s (c) k=3, 5966 samples, 14min 56s

Figure 4.5: EGDIS selected samples by varying the hyper-parameter k. The score distributions show that EGDIS selects samples from both high score region and low score region.

The drawback of EGDIS is the global density calculation which computes the distance between all training samples. In our experiments, it took us on average 14 minutes 50 seconds to get all the selected samples, and we only need about 12 seconds to select the boundary samples. Figure 4.6 shows the score distribution of EDGIS selected boundary samples with $k = 3$. Compared with the second column of Figure 4.5(c), the main difference is the lack of high score samples. Therefore, if we choose to select higher score samples from the score list, we can combine them with EGDIS selected boundary samples and get a similar EGDIS score distribution within about 20 seconds. We will mention this topic in the next few paragraphs.

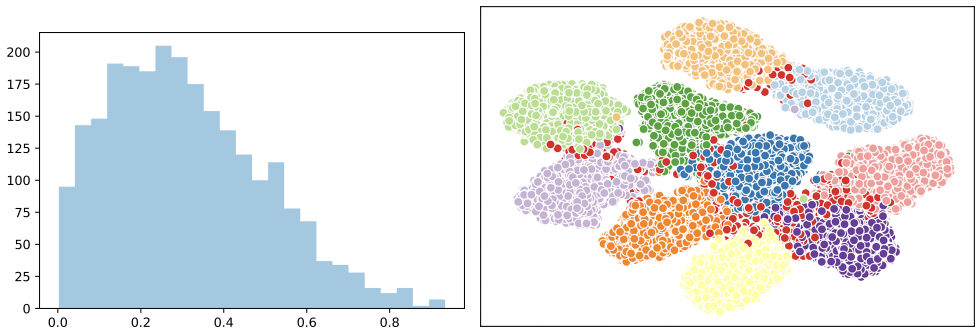

(a) Score distribution (b) Selected samples

Figure 4.6: EGDIS boundary score distribution and selected samples.

Next, we visualised the selection preference of CL in Figure 4.7. We selected different percentages of samples, and the selection pattern is distinct from POP and EGDIS. We can see that CL tends to select only high score samples, and these samples are lying in the opposite direction as the EGDIS boundary samples. This result is what we expected because samples far from the decision boundary would have high scores for the linear classifier. From the score distributions, we can see that all selected samples are easy to classify for deep learning. This discovery reminds us to combine these high score samples with EGDIS boundary samples. From Figure 4.7 and 4.6, we can construct the bound of the blobs. However, the downside is that no inner samples are selected, and the borders are not complete. We can not capture the whole shape of the blobs, and the results are more like two isolated blobs for each class. With a linear regression model, the boundary cannot be recovered precisely so we may get lower accuracy.

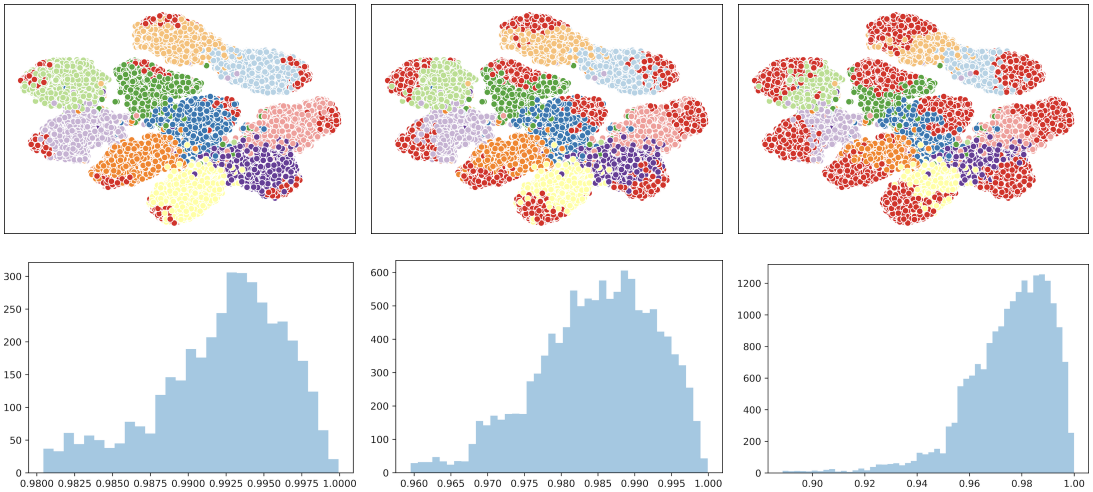

(a) P=10%, 4000 samples (b) P=30%, 12000 samples (c) P=50%, 20000 samples

Figure 4.7: CL selected samples by tuning the percent of samples to select.

Rather than selecting only the top score samples, we proposed WCL to randomly select samples within each class based on the sample scores. The results are shown in the first row of Figure 4.8. Although most samples are selected from the high score regions, there are some samples selected from the lower score regions. The problem is that fewer samples near the EGDIS boundary are chosen. The boundary between close blobs are blurry thus we cannot guarantee the performance.

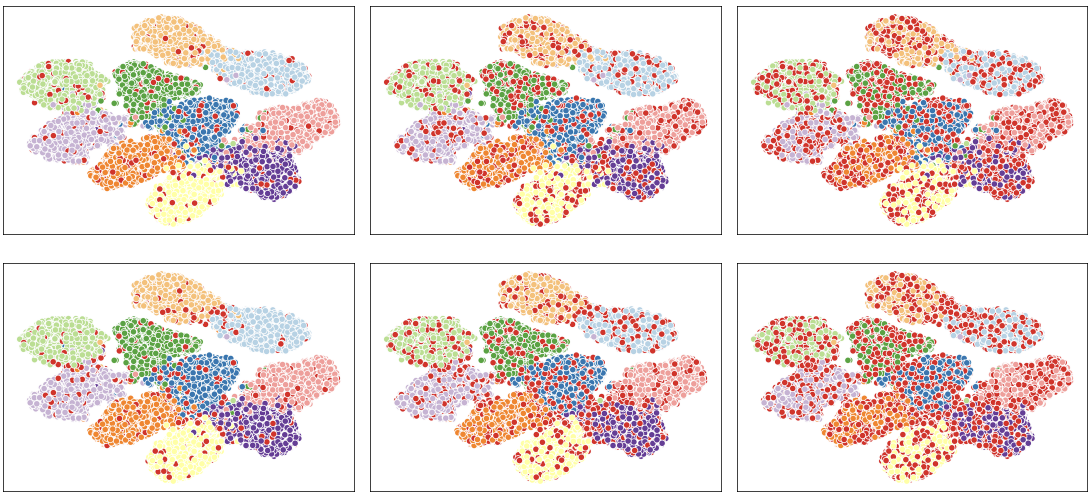

(a) P=10%, 4000 samples (b) P=30%, 12000 samples (c) P=50%, 20000 samples

Figure 4.8: WCL selected samples by tuning selection percentage. The first row we use weighted sampling method, the second row we use EGDIS boundary based method.

Therefore, we combined both WCL and EGDIS selected boundary samples to propose the method BWCL. Compared with EGDIS, our BWCL can both get a similar score distribution as well as recover the shape of blobs. However, due to the randomness during selection, we cannot guarantee to select the same datasets each time. This characteristic may cause the classification accuracy unstable for machine learning models. We plotted the score distributions in Figure 4.9. We found that the score distribution of WCL is similar with the score distribution of the whole dataset in Figure 4.3 while by selecting a close amount of samples, BWCL score distributions are similar with EGDIS in Figure 4.5(c).

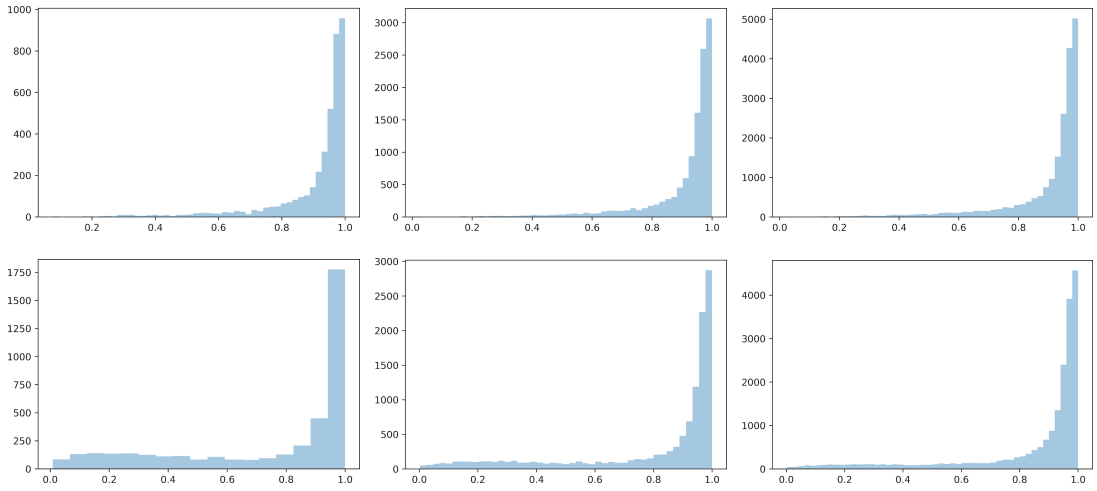

(a) P=10%, 4000 samples (b) P=30%, 12000 samples (c) P=50%, 20000 samples

Figure 4.9: WCL and BWCL score distributions by tuning selection percentage. The first row we use WCL, the second row we use BWCL.

4.3 Experiment 3: Logistic Regression

For more comprehensive evaluation results and inspired by [20], we manually synthesised two CIFAR100 subsets and filled in the classification gap between CIFAR10 and CIFAR100. Between 10 classes to 90 classes with gap 10, we choose to build nine subsets with by selecting the samples from the required number of classes. For each required classes, we randomly did the job five times and trained them to convergence with the logistic regression model. The box plot is shown in Figure 4.10. We chose 40 classes and 20 classes as the number of our new synthesised datasets, with test accuracy 0.78925 and 0.853. They have 8,028 samples and 16042 samples respectively. Then we repeated the feature compression process described in Section 4.1 to compress the extracted features. The final test accuracy is 0.8065 and 0.8745. In our reported accuracy below, we used CIFAR20 and CIFAR40 to refer to these synthesised datasets.

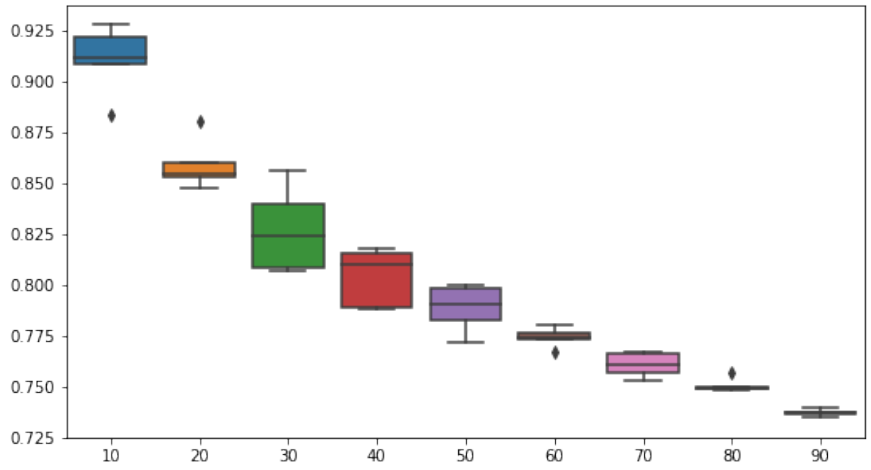

Figure 4.10: The test set accuracies of CIFAR100 subsets. Horizontal axis is the number of classes selected. Vertical axis is the accuracy score. For each selection, we randomly choose the classes for five times and report the accuracy with logistic regression model.

Our first discovery is that it is hard to select the right amount of subsets with POP because the number of samples with weakness 128 is very low for all datasets except CIFAR10. Even for equal threshold 1, the number of pure inner is still low. Therefore, it is not good to choose samples with weakness < 128. From our experiment, we found that the reduction rate for EGDIS is good enough. Therefore, we make POP, CL, WCL and BWCL to select the same amount of samples as EGDIS. For POP, we ranked samples based on weakness and select from low to high. Therefore, we can have a fair comparison of their classification performance. The POP weakness distributions are shown in Figure 4.11.

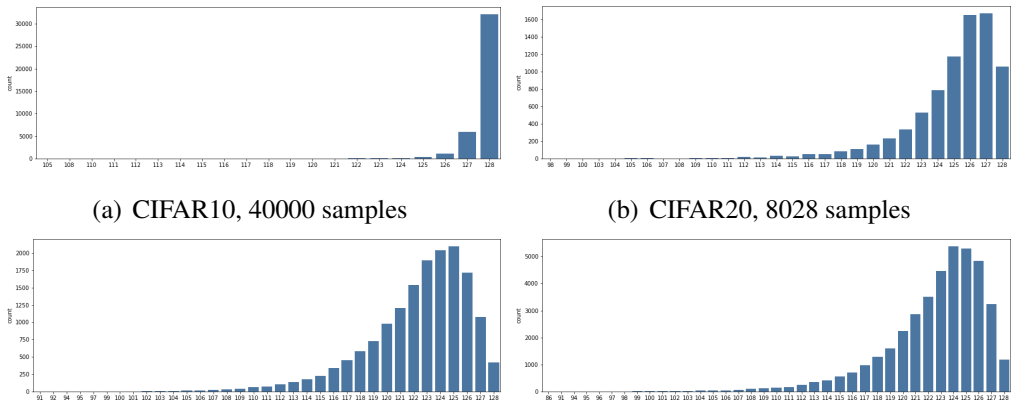

(a) CIFAR10, 40000 samples

(b) CIFAR20, 8028 samples

(c) CIFAR40, 16042 samples

(d) CIFAR100, 40000 samples

Figure 4.11: POP weakness distributions for the 4 datasets. The very right column is the number of pure inner samples. We can see that the heights are lower except for CIFAR10.

For the five algorithms, we performed the selection process 12 times and reported the average accuracy with the logistic regression model. The relative accuracy is recorded in Table 4.1. We can see that the retention rate [1] is increasing with the classification difficulty of the datasets. POP and EGDIS performed better with simpler dataset such as CIFAR10. For EGDIS, it even achieved an accuracy increase. We think this is because with selected boundary and dense samples only, the overfitting problem is reduced. However, the performances of WCL and BWCL are more stable than EGDIS. Their relative accuracy decreases slowly just like POP. Among all three classification score based algorithms, BWCL is more capable of dealing with harder datasets. We believe the reason is that BWCL can maintain the EGDIS selected boundary and the WCL self-adaptive selection manner benefits the classification accuracy. The original accuracies are recorded in Table A.1.

Datasets	Retention Rate	POP	EGDIS	CL	WCL	BWCL
CIFAR10	14.915%	100.00%	**100.04**%	99.74%	99.96%	99.91%
CIFAR20	16.67%	**99.94**%	99.01%	99.57%	99.31%	99.43%
CIFAR40	21.09%	**99.64**%	98.92%	99.09%	99.46%	99.63%
CIFAR100	31.48%	99.38%	97.78%	98.78%	99.46%	**99.49**%

Table 4.1: Logistic Regression test set relative accuracy by averaging 12 runs

We should notice that the average relative accuracy of BWCL is not the best value.

[1] Retention rate is the proportion of samples selected.

We tuned the maximum proportion of boundary samples from 0.1 to 0.4 with step 0.1 and trained them three times each. In Figure 4.14(b), we reported the relative accuracy in plot. It is clear that for simpler datasets, we should choose less hard examples. For harder datasets, we should choose more boundary samples.

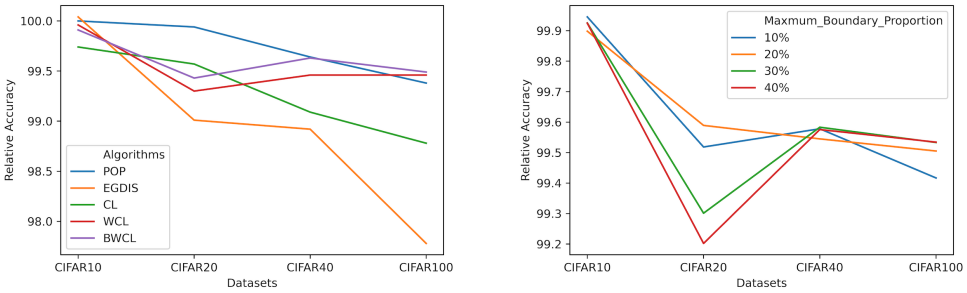

(a) Relative Accuracy

(b) Relative Accuracy of BWCL by tuning maximum boundary proportion

Figure 4.12: Relative Accuracy of data reduction algorithms

We took a further analysis for BWCL, by varying the proportion of samples selected relative to the number of samples selected by EGDIS. We fixed the maximum boundary proportion to 10%. The relative accuracy is reported in Figure 4.13. We found that the quality of the extracted features are so good that the test set samples are classified easily. This means that the results from logistic regression may not transfer to CNN experiments well but this provides us with a good start.

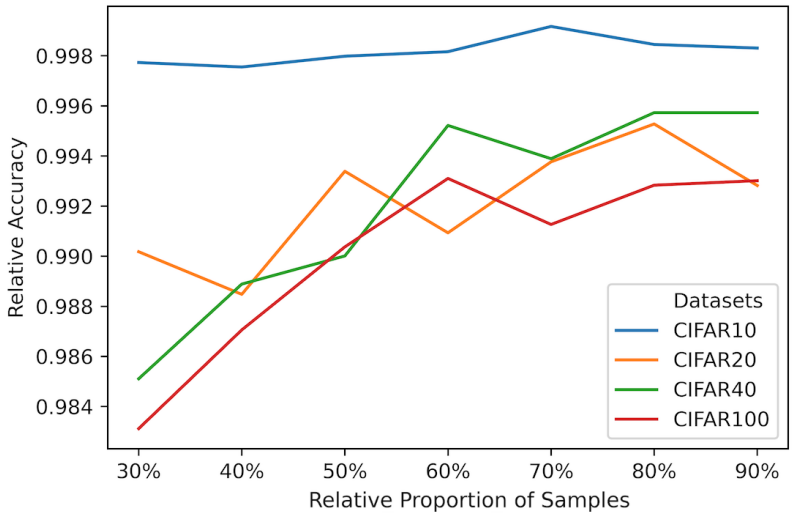

Figure 4.13: The BWCL test set accuracies. Averaged with 3 individual runs. The threshold is 10%. Horizontal axis is the percentage of samples selected, in term of EDGIS selected samples. Vertical axis is the accuracy score.

4.4 Experiment 4: Instance Selection for CNN

We trained the network DenseNet121 for three times, with learning rate 0.1 (150 epochs), 0.01 (100 epochs) and 0.001 (100 epochs). First, we trained the network with the same selection configuration as logistic regression and reported the classification accuracy in Table 4.2. The original accuracies are shown in Table A.3.

Datasets	Retention Rate	POP	EGDIS	CL	WCL	BWCL
CIFAR10	14.915%	86.80%	85.18%	86.71%	**88.36%**	86.75%
CIFAR20	16.67%	59.93%	61.43%	**70.96%**	69.34%	64.67%
CIFAR40	21.09%	63.99%	63.89%	**75.77%**	71.36%	70.65%
CIFAR100	31.48%	75.24%	73.74%	82.72%	**83.23%**	81.69%

Table 4.2: CNN test set relative accuracy

First of all, we found that POP and EGDIS selected samples are not suitable for a neural network. The network cannot extract good features from these images thus the relative accuracy is much lower than expected. Second, classification score based algorithms can achieve relatively higher accuracy. In particular, for datasets with less per-class samples, CL is better. For datasets with more per-class samples, WCL is better.

However, BWCL performs worse than expected. We tested the BWCL performance by tuning the maximum EGDIS boundary proportion. The results are shown in Figure 4.14(b). It seems that we should not set the proportion hyper-parameter larger than 10%. We believe this is because we evaluated the classification scores with NasNet-Large, who has better extraction power than DenseNet121. The subsets contained too many hard examples so the network cannot handle the training samples well. We proposed another hypothesis that if the network could learn these hard samples well, then it should be able to achieve higher classification accuracy based on the hard-example mining method described in Chapter 2.

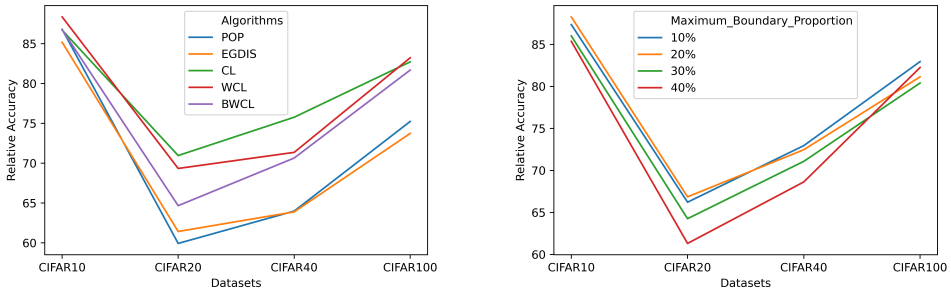

(a) Relative Accuracy

(b) Relative Accuracy of BWCL by tuning maximum boundary proportion

Figure 4.14: Relative Accuracy of data reduction algorithms

We took a closer look at the training curve of the first training stage to analysis the convergence speed. For all datasets, CL and WCL can select samples to help the network to converge faster. For BWCL, it can speed up the training process for CIFAR100. However, for CIFAR20, BWCL may even slow down the convergence speed. The discovery indicates that BWCL is much difficult to tune compared with CL and WCL.

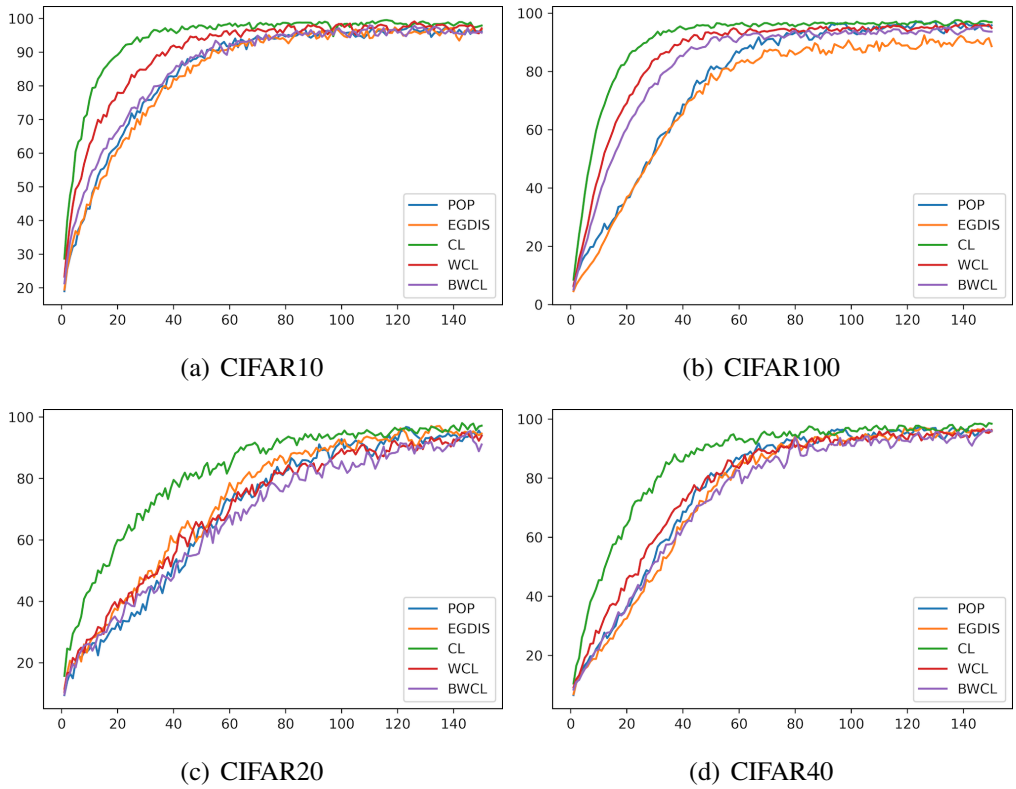

(a) CIFAR10 (b) CIFAR100

(c) CIFAR20 (d) CIFAR40

Figure 4.15: The training trend of four datasets by selecting the same amount of samples as EGDIS, of the first 150 epochs

We took a closer look at the relative accuracy achieved by adjusting the proportion of samples selected by these algorithms. It seems that WCL is better than CL and BWCL when dealing with easier datasets such as CIFAR10. For other datasets, WCL is more stable because the curves are close to straight lines. However, we still have one more problem remains: how to set the right amount of samples to select as a start? We noticed that for all our four datasets, by selecting 50% of the whole samples, we can have a relative accuracy higher than 90%. A heuristic guide is to take 50% of samples and consider it as 90% relative accuracy. Then use a linear model to decide the number of samples to select. To make this more reliable, we took another experiment, by analysing the relationship between validation accuracy history and final relative accuracy. We reported the detail in the next Chapter.

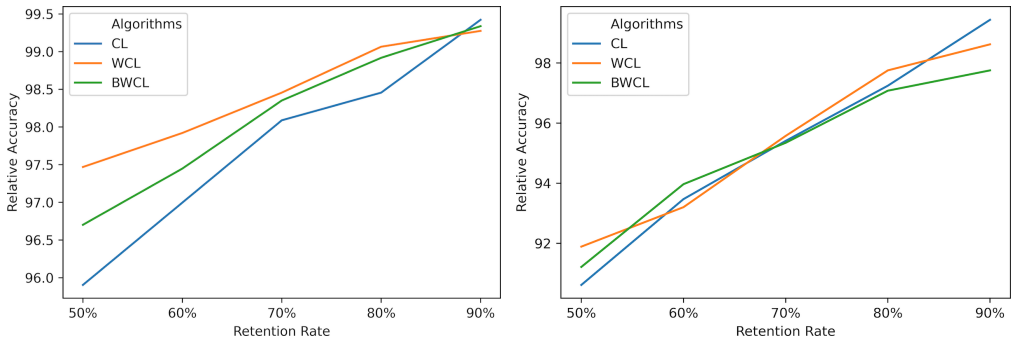

(a) CIFAR10 (b) CIFAR100

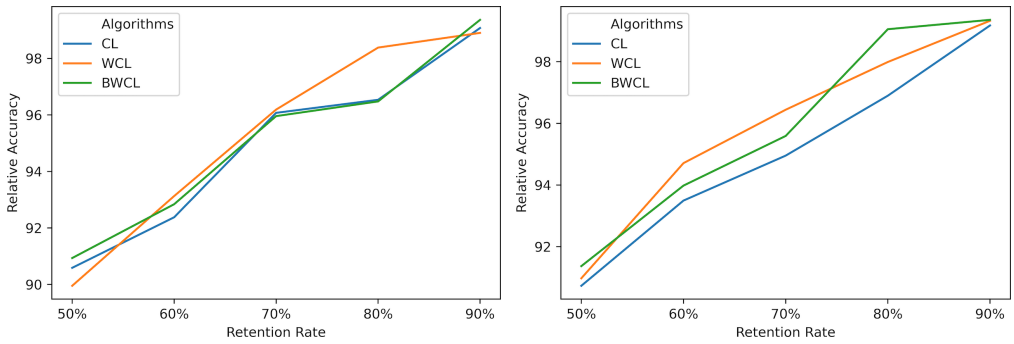

(c) CIFAR20 (d) CIFAR40

Figure 4.16: The relative accuracy to compare the performance of three algorithms with different retention rate.

4.5 Conclusion

Although POP is fast than EGDIS, it not suitable for datasets with a large number of feature dimensions. All five algorithms can achieve relative accuracies higher than 95% for logistic regression classifier because the extracted features are easy to classify. For CNNs, CL and WCL perform better. In particular, WCL works well for datasets with more samples. An unexpected result is that BWCL performs worse than CL and WCL. A possible reason is that the selected hard samples are beyond the ability of DenseNet121. Therefore, we suggest using the extracted features directly if the task does not need original images. For cases when training the network is necessary, WCL should be the first choice if the dataset has a large number of samples. For researchers who want to explore a new network structure which may be able to learn from hard samples, BWCL may be the right choice.

Chapter 5

Trade-off Framework

A useful trade-off framework should be able to help the researchers to decide how much samples they need for a given relative accuracy such as BlinkML [32]. Since Istrate et al. [20] shows that the CNN classification accuracies can be predicted from training experiment histories, we should be able to build such a framework with enough training experiment histories. In our project, we failed to collect enough data for the instance selection algorithms because of the lack of computing resources. Therefore, we tend to provide a general framework which is not dependent on a particular instance selection algorithm. In this way, we got 240 samples for CIFAR10 and 88 samples for CIFAR100. These training histories are from the experiment result in Chapter 4. Our framework consists of three stages:

1. We first select the subset with a particular instance selection algorithm and train the subset for 10 epochs.

2. Then the framework predicts whether this subset could achieve a relative accuracy above 90% or not.

3. If it can achieve above 90%, the framework predicts the relative accuracy.

According to the trainless accuracy predictor published by IBM [36], the validation accuracy form the first few epochs of a smaller network are linearly related to the final test accuracy. If their experiment is reliable, we could expect it works for relative accuracy as well, for a particular dataset. Also, we want to know if this works for other networks, such as DenseNet121 so we don't need extra training task. We plotted the results in Figure 5.3 to analyse this hypothesis. We did not use CIFAR20 and CIFAR40 history because we want to focus on large datasets. The result is not precisely linear

in our case. The shape is more like part of an arc curve instead. However, if we zoom in the region where relative accuracy is bigger than 0.9, the curve is more close to a linear line, especially for CIFAR10.

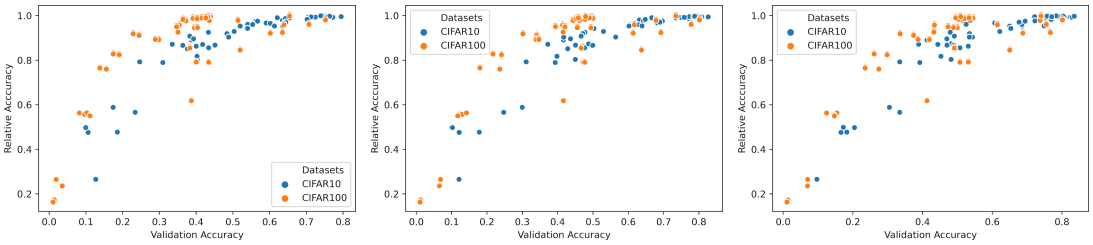

(a) Epoch 5 (b) Epoch 7 (c) Epoch 9

Figure 5.1: The linear relationship between the validation accuracy and the final relative accuracy achieved

We also explored the logit transformation method recommended by Kornblith et al. [23]. This transformation scales the accuracy with the equation $log(\frac{Validation\ Accuracy}{1-Validation\ Accuracy})$. In Figure 5.2, we can see that the relationship is very close to linear. This result is close to the relative accuracy predictor that we want. However, a single linear model with only one input is not precise enough for our framework. We discussed the framework design in Section 5.1 in more detail.

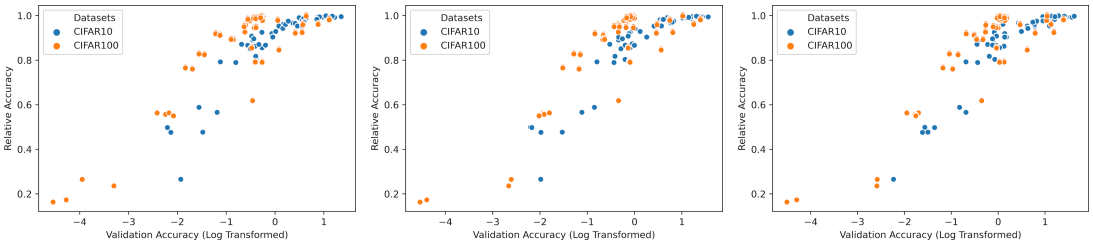

(a) Epoch 5 (b) Epoch 7 (c) Epoch 9

Figure 5.2: The linear relationship between the validation accuracy and the final relative accuracy achieved

5.1 Trade-off Framework Design

Although we discovered the linear relationship between the first few epoch validation accuracies and the relative accuracy achieved in the end, the linear curve is still not good enough. Therefore, we decided to use machine learning methods to get a better prediction result. The sixteen features we chose to train with are:

1. the retention rate
2. the subset validation accuracies for the first ten epochs
3. the whole dataset validation accuracies for the first five epochs

To summary, we trained two models individually as follows:

1. We first train a classifier to decide if the selected epochs can achieve at least 90% relative accuracy or not.
2. We then train a regression model to predict the final relative accuracy for subsets that achieved a relative accuracy higher than 90%.

5.1.1 Performance Evaluation

We split the history set into a training set and a test set with ratio 8:2. Our classifier easily achieved 100% test accuracy for CIFAR10 and 94.44% for CIFAR100. The relative accuracy predictor achieved a R2 score 0.9635 for CIFAR10 and 0.7920 for CIFAR100. By selecting only samples with accuracy larger than 90%, we got good linear results shown in Figure 5.3.

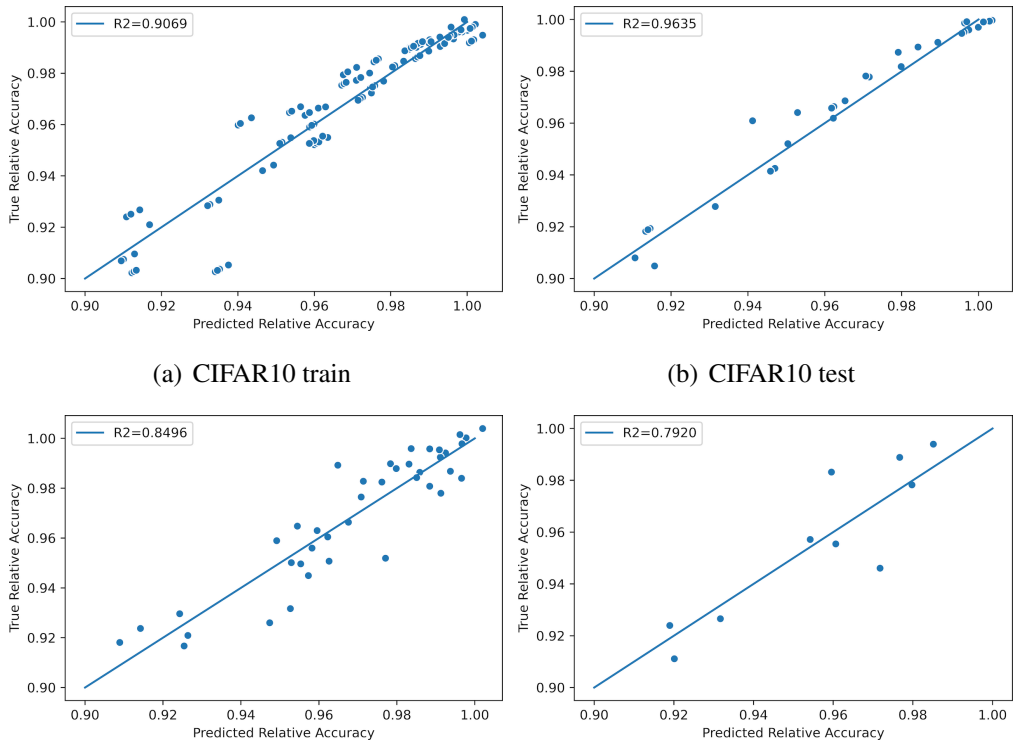

(a) CIFAR10 train (b) CIFAR10 test

(c) CIFAR100 train (d) CIFAR100 test

Figure 5.3: The linear model for CIFAR10 and CIFAR100 to predict the relative accuracy

Although the predicted relative accuracy results are precise, we cannot guarantee the framework works well for other datasets. The R2 score decreases for CIFAR100 compared with CIFAR10. We have the reason to believe the score would be lower for the dataset which is harder to classify than CIFAR100. Also, since we do not have plenty of samples, the regression model may not capture the actual patterns. We will discuss possible improvements in Chapter 6.

Chapter 6

Conclusion and Future Work

We evaluated three existing instance selection algorithms, POP [34], EGDIS [34], CL [16], and proposed two variations, WCL and BWCL, on CIFAR10 and CIFAR100 in this project. We chose to use pre-trained network NasNetLarge [43] to extract image features as a pre-processing step and compressed the feature vectors by training two FC layers. We compared their selection preferences by visualising the selected samples with t-SNE and tuned the hyper-parameters to analyse the algorithms further. Then we compared the relative accuracies achieved by the logistic regression model as well as the network DenseNet121. At the end of Chapter 4, we summarised the evaluation results and gave suggestions to choose the proper one based on different situations. In short, POP and EGDIS are suitable for machine learning algorithms such as logistic regression. CL and WCL work better when retraining a network is necessary. BWCL is a special one and it can be used to design new network structures. We also developed a trade-off framework which can guide the researchers to choose the number of samples to keep for CL, WCL and BWCL in particular because they need to know the number of samples needed.

There are several limitations in our evaluation: we omitted the fine-tuning process to extract better feature vectors. We did not have enough time to evaluate more datasets and more CNN structures. Also, we did not evaluate the performance of other deep learning tasks other than image classification. From our perspective, the pipeline we described in Chapter 3 may be able to work with other vision datasets like video or 3D model if we could find a way to describe the samples with structured features. However, we did not have any related knowledge when designing this project so we will leave this challenge to the future.

In addition, we could extend the trade-off framework to handle different require-

ments. For example, we may want to predict how many more samples needed to achieve a required accuracy based on a given subset. According to the Google Data Labelling Service [1], it costs 35$ to label 50,000 images for classification tasks. The price goes to 870$ for segmentation tasks. It would cost a lot to build large datasets with millions of images. If we could train the framework to do this task, we may save the sponsor a huge amount of money. Moreover, our framework treats datasets individually. We have not found a way to handle different datasets with a single model even with neural networks. The performance would be worse than the results described in Chapter 5. Since TAPAS [20] has proved the feasibility to learn from training histories, we should be able to build such a framework in the future.

Bibliography

[1] AI Platform Data Labeling Service. https://cloud.google.com/ai-platform/data-labeling/docs, last accessed on 21/08/2020.

[2] TensorFlow Hub. NasNetLarge. https://tfhub.dev/google/imagenet/nasnet_large/feature_vector/4, last accessed on 21/08/2020.

[3] David W. Aha, Dennis Kibler, and Marc K. Albert. Instance-based learning algorithms. *Machine Learning*, 6(1):37–66, jan 1991.

[4] Saleh Albelwi and Ausif Mahmood. Analysis of instance selection algorithms on large datasets with Deep Convolutional Neural Networks. In *2016 IEEE Long Island Systems, Applications and Technology Conference, LISAT 2016*. Institute of Electrical and Electronics Engineers Inc., jun 2016.

[5] Yoshua Bengio, Jérome Louradour, Ronan Collobert, and Jason Weston. Curriculum learning. In *ACM International Conference Proceeding Series*, volume 382, pages 1–8, New York, New York, USA, 2009. ACM Press.

[6] Vighnesh Birodkar, Hossein Mobahi, and Samy Bengio. Semantic Redundancies in Image-Classification Datasets: The 10% You Don't Need. jan 2019.

[7] Lukas Bossard, Matthieu Guillaumin, and Luc Van Gool. Food-101 - Mining discriminative components with random forests. In *Lecture Notes in Computer Science (including subseries Lecture Notes in Artificial Intelligence and Lecture Notes in Bioinformatics)*, volume 8694 LNCS, pages 446–461. Springer Verlag, 2014.

[8] Henry Brighton and Chris Mellish. Advances in instance selection for instance-based learning algorithms, 2002.

[9] Haw Shiuan Chang, Erik Learned-Miller, and Andrew McCallum. Active bias: Training more accurate neural networks by emphasizing high variance samples.

In *Advances in Neural Information Processing Systems*, volume 2017-Decem, pages 1003–1013, 2017.

[10] Yushi Chen, Hanlu Jiang, Chunyang Li, Xiuping Jia, and Pedram Ghamisi. Deep Feature Extraction and Classification of Hyperspectral Images Based on Convolutional Neural Networks. *IEEE Transactions on Geoscience and Remote Sensing*, 54(10):6232–6251, oct 2016.

[11] Mircea Cimpoi, Subhransu Maji, Iasonas Kokkinos, Sammy Mohamed, and Andrea Vedaldi. Describing textures in the wild. In *Proceedings of the IEEE Computer Society Conference on Computer Vision and Pattern Recognition*, pages 3606–3613. IEEE Computer Society, sep 2014.

[12] Gabriella Csurka, Christopher R Dance, Lixin Fan, Jutta Willamowski, and Cédric Bray. Visual Categorization with Bags of Keypoints. In *Workshop on statistical learning in computer vision, ECCV*, pages 1(1–22): 1–2, 2004.

[13] Xavier Glorot and Yoshua Bengio. Understanding the difficulty of training deep feedforward neural networks. In *Journal of Machine Learning Research*, volume 9, pages 249–256, 2010.

[14] Ian Goodfellow, Yoshua Bengio, and Aaron Courville. *Deep Learning*. 2016.

[15] Ian Goodfellow, Yoshua Bengio, Aaron Courville, and Yoshua Bengio. *Deep learning*, volume 1. MIT press Cambridge, 2016.

[16] Guy Hacohen and Daphna Weinshall. On the power of curriculum learning in training deep networks. In *36th International Conference on Machine Learning, ICML 2019*, volume 2019-June, pages 4483–4496, 2019.

[17] Kaiming He, Xiangyu Zhang, Shaoqing Ren, and Jian Sun. Delving deep into rectifiers: Surpassing human-level performance on imagenet classification. In *Proceedings of the IEEE International Conference on Computer Vision*, volume 2015 Inter, pages 1026–1034, 2015.

[18] Kaiming He, Xiangyu Zhang, Shaoqing Ren, and Jian Sun. Deep residual learning for image recognition. In *Proceedings of the IEEE Computer Society Conference on Computer Vision and Pattern Recognition*, volume 2016-Decem, pages 770–778, 2016.

[19] Gao Huang, Zhuang Liu, Laurens van der Maaten, and Kilian Q. Weinberger. Densely Connected Convolutional Networks. In *Proceedings - 30th IEEE Conference on Computer Vision and Pattern Recognition, CVPR 2017*, volume 2017-Janua, pages 2261–2269. Institute of Electrical and Electronics Engineers Inc., aug 2016.

[20] R. Istrate, F. Scheidegger, G. Mariani, D. Nikolopoulos, C. Bekas, and A. C. I. Malossi. TAPAS: Train-Less Accuracy Predictor for Architecture Search. *Proceedings of the AAAI Conference on Artificial Intelligence*, 33:3927–3934, jun 2019.

[21] Angelos Katharopoulos and François Fleuret. Biased Importance Sampling for Deep Neural Network Training. may 2017.

[22] Angelos Katharopoulos and François Fleuret. Not All Samples Are Created Equal: Deep Learning with Importance Sampling. *35th International Conference on Machine Learning, ICML 2018*, 6:3936–3949, mar 2018.

[23] Simon Kornblith, Jonathon Shlens, and Quoc V. Le. Do better imagenet models transfer better? In *Proceedings of the IEEE Computer Society Conference on Computer Vision and Pattern Recognition*, volume 2019-June, pages 2656–2666, may 2019.

[24] Alex Krizhevsky. Learning multiple layers of features from tiny images. Technical report, 2009.

[25] Alex Krizhevsky, Ilya Sutskever, and Geoffrey E Hinton. ImageNet classification with deep convolutional neural networks. *Communications of the ACM*, 60(6):84–90, 2017.

[26] M. Pawan Kumar, Benjamin Packer, and Daphne Koller. Self-paced learning for latent variable models. In *Advances in Neural Information Processing Systems 23: 24th Annual Conference on Neural Information Processing Systems 2010, NIPS 2010*, pages 1189–1197, 2010.

[27] Hao Li and Maoguo Gong. Self-paced Convolutional Neural Networks. Technical report, 2017.

[28] Ilya Loshchilov and Frank Hutter. Online Batch Selection for Faster Training of Neural Networks. nov 2015.

[29] Mohamed Malhat, Mohamed El Menshawy, Hamdy Mousa, and Ashraf El Sisi. A new approach for instance selection: Algorithms, evaluation, and comparisons. *Expert Systems with Applications*, 149:113297, jul 2020.

[30] Deyu Meng, Qian Zhao, and Lu Jiang. What Objective Does Self-paced Learning Indeed Optimize? 2015.

[31] J Arturo Olvera-López, J. Ariel Carrasco-Ochoa, J. Francisco Martínez-Trinidad, and Josef Kittler. A review of instance selection methods, 2010.

[32] Yongjoo Park, Jingyi Qing, Xiaoyang Shen, and Barzan Mozafari. BlinkML: Efficient maximum likelihood estimation with probabilistic guarantees. In *Proceedings of the ACM SIGMOD International Conference on Management of Data*, pages 1135–1152, New York, New York, USA, jun 2019. Association for Computing Machinery.

[33] Vlad Popovici and Jean Philippe Thiran. Face Detection Using an SVM Trained in Eigenfaces Space. *Lecture Notes in Computer Science (including subseries Lecture Notes in Artificial Intelligence and Lecture Notes in Bioinformatics)*, 2688:190–198, 2003.

[34] José C. Riquelme, Jesús S. Aguilar-Ruiz, and Miguel Toro. Finding representative patterns with ordered projections. *Pattern Recognition*, 36(4):1009–1018, apr 2003.

[35] Olga Russakovsky, Jia Deng, Hao Su, Jonathan Krause, Sanjeev Satheesh, Sean Ma, Zhiheng Huang, Andrej Karpathy, Aditya Khosla, Michael Bernstein, Alexander C. Berg, and Li Fei-Fei. ImageNet Large Scale Visual Recognition Challenge. *International Journal of Computer Vision*, 115(3):211–252, dec 2015.

[36] Florian Scheidegger, Roxana Istrate, Giovanni Mariani, Luca Benini, Costas Bekas, and Cristiano Malossi. Efficient Image Dataset Classification Difficulty Estimation for Predicting Deep-Learning Accuracy. mar 2018.

[37] Abhinav Shrivastava, Abhinav Gupta, and Ross Girshick. Training region-based object detectors with online hard example mining. In *Proceedings of the IEEE Computer Society Conference on Computer Vision and Pattern Recognition*, volume 2016-Decem, pages 761–769, 2016.

[38] Wei Song, Lingfeng Zhang, Yifei Tian, Simon Fong, Jinming Liu, and Amanda Gozho. CNN-based 3D object classification using Hough space of LiDAR point clouds. *Human-centric Computing and Information Sciences*, 10(1):1–14, dec 2020.

[39] Xunhu Sun and Philip K. Chan. An analysis of instance selection for neural networks to improve training speed. In *Proceedings - 2014 13th International Conference on Machine Learning and Applications, ICMLA 2014*, pages 288–293. Institute of Electrical and Electronics Engineers Inc., feb 2014.

[40] Laurens van der Maaten and Geoffrey Hinton. Visualizing Data using t-SNE. *Journal of Machine Learning Research*, 9:2579–2605, 2008.

[41] Peng Xu, Fred Roosta, and Michael W Mahoney. Second-order optimization for non-convex machine learning: An empirical study. In *Proceedings of the 2020 SIAM International Conference on Data Mining, SDM 2020*, pages 199–207, 2020.

[42] Peilin Zhao and Tong Zhang. Stochastic optimization with importance sampling for regularized loss minimization. In *32nd International Conference on Machine Learning, ICML 2015*, volume 1, pages 1–9, 2015.

[43] Barret Zoph, Vijay Vasudevan, Jonathon Shlens, and Quoc V. Le. Learning Transferable Architectures for Scalable Image Recognition. In *Proceedings of the IEEE Computer Society Conference on Computer Vision and Pattern Recognition*, pages 8697–8710. IEEE Computer Society, jul 2018.

Appendix A

Training History

A.1 Feature Extraction for CIFAR20 and CIFAR40

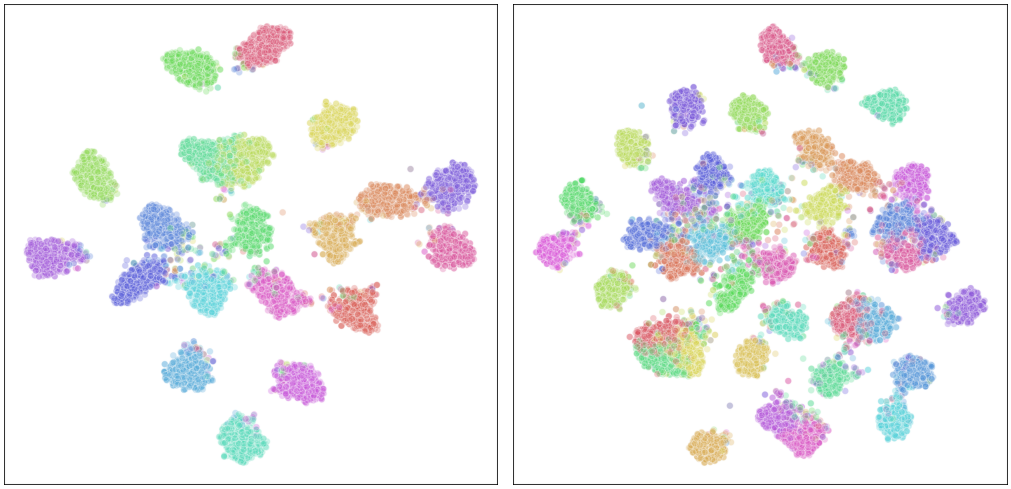

(a) CIFAR20 (b) CIFAR40

Figure A.1: Extracted features visualisation with t-SNE algorithm

A.2 Logistic Regression Original History

Datasets	Retention Rate	Whole	POP	EGDIS	CL	WCL	BWCL
CIFAR10	14.915%	0.9258	0.9258	**0.9262**	0.9234	0.9254	0.9250
CIFAR20	16.67%	0.8825	**0.8820**	0.8738	0.8787	0.8764	0.8775
CIFAR40	21.09%	0.8159	**0.8130**	0.8071	0.8085	0.8115	0.8129
CIFAR100	31.48%	0.7444	0.7398	0.7279	0.7353	0.7404	**0.7406**

Table A.1: Logistic Regression test set accuracy by averaging 12 runs

Datasets	Retention Rate	10%	20%	30%	40%
CIFAR10	14.915%	**0.9253**	0.9249	0.9246	0.9251
CIFAR20	16.67%	0.8783	**0.8789**	0.8758	0.8744
CIFAR40	21.09%	0.8125	0.8122	**0.8134**	0.8132
CIFAR100	31.48%	0.7401	0.7407	**0.7410**	**0.7410**

Table A.2: Logistic Regression BWCL test set accuracy by averaging 12 runs

A.3 CNN Original History

Datasets	Retention Rate	Whole	POP	EGDIS	CL	WCL	BWCL
CIFAR10	14.915%	0.9522	0.8265	0.8111	0.8257	**0.8414**	0.8260
CIFAR20	16.67%	0.8660	0.5190	0.5320	**0.6145**	0.6005	0.5600
CIFAR40	21.09%	0.8233	0.5268	0.5260	**0.6238**	0.5875	0.5816
CIFAR100	31.48%	0.7842	0.5900	0.5783	0.6487	**0.6527**	0.6406

Table A.3: CNN test set accuracy

Datasets	Retention Rate	10%	20%	30%	40%
CIFAR10	14.915%	0.8318	**0.8405**	0.8189	0.8128
CIFAR20	16.67%	0.5735	**0.5790**	0.5565	0.5310
CIFAR40	21.09%	**0.5953**	0.5913	0.5800	0.5600
CIFAR100	31.48%	**0.6505**	0.6363	0.6305	0.6450

Table A.4: BWCL test set accuracy